

MAXIMIZING THE SIGNAL-TO-NOISE RATIO OF THE ELECTROMAGNETIC SEISMOMETER: THE OPTIMUM COIL RESISTANCE, AMPLIFIER CHARACTERISTICS, AND CIRCUIT

BY PETER W. RODGERS

ABSTRACT

This study finds the optimum coil resistance, $r_{c,opt}$, which maximizes the signal-to-noise ratio (SNR) of an electromagnetic (EM) seismometer and amplifier combination. The optimum coil resistance is shown to be the product of a seismometer factor (SF) times the noise resistance, R_n , of the amplifier. The seismometer factors range from 1.13 to 3.66 for the nine EM seismometers considered. The minimum noise figure solution, in which the amplifier noise resistance is set equal to the coil resistance, is shown to correspond to the special case in which there is no damping resistor present. It is also shown that the optimum form for the noise resistance is a constant independent of frequency and that this feature can be approximated with FET-like components such as the MAT-02. Examples of using $r_{c,opt}$ are given using both the 5500-ohm and the 500-ohm 1-Hz L4-C seismometers paired with the OP-27 and LT1028 operational amplifiers, respectively. It is pointed out that, although the resulting amplitude signal-to-noise ratios (ASNRs) are approximately equal, it is best to choose the seismometer-amplifier pair having the larger generator constant because it results in a larger signal. Furthermore, if the coil resistance is not the optimum value, the resulting decrease in the ASNR is less if the coil resistance is chosen greater than the optimum rather than less.

The deleterious effects of mismatching seismometer and amplifier are shown by comparing ASNRs for the GS-13 seismometer paired with three different amplifiers. The degradation in ASNR is found to be as large as a factor of 3. It is pointed out that mismatching would not be done purposely but can inadvertently occur when connecting an EM seismometer to a seismic recorder whose input noise resistance properties are unknown, as is generally the case. It is recommended that manufacturers of seismic recorders obtain the necessary input noise data from the component manufacturers and supply the input noise resistance to users.

Finally, the three commonly used single-ended preamplifier circuits used for EM seismometers are compared in terms of their resulting ASNRs. The same seismometer and amplifier are used in all three circuits. For the GS-13 / MAT-02 pair, the noninverting, parallel damping resistor circuit resulted in an ASNR that was 3.8 times larger than that for the inverting, parallel damping resistor circuit, and 3 times larger than that for the inverting, series damping resistor circuit.

INTRODUCTION

Most electromagnetic (EM) seismometers are available with a range of different coil resistances and generator constants. In deciding which to select, there is always the question of whether to choose the unit having a large generator constant and accompanying larger coil resistance, which means more electronic noise, or to choose the unit with a smaller generator constant and smaller coil resistance resulting in a smaller signal, but also smaller electronic noise. This

* Present address: PETER W. RODGERS, 1530 TWINRIDGE ROAD, SANTA BARBARA, CA 93111

work addresses that question in general by showing that there is a coil resistance that maximizes the signal while minimizing the three types of electronic noise together with the suspension noise. In other words, for a given seismometer and preamplifier combination, an expression for the coil resistance is found that maximizes the signal-to-noise ratio (SNR). It also follows that there is an amplifier characteristic that maximizes the SNR for a given coil resistance.

That there may be such an optimum coil resistance is suggested by the result of minimizing the noise figure (NF) of an amplifier (Horowitz and Hill, 1989, Chapter 7). This result shows that, for a fixed source resistance, the amplifier-induced electronic noise at the input of an amplifier is minimized by selecting an amplifier whose noise resistance, R_n , is equal to the given source resistance. The terms noise figure and amplifier noise resistance will be defined in detail later. The implications of the minimum NF analysis in choosing an operational amplifier (op-amp) to minimize the amplifier-induced electronic noises with a given coil resistance are discussed by Riedesel *et al.* (1990). They correctly point out that the electronic noise is reduced by pairing a low R_n operational amplifier with a low coil resistance and a high R_n op-amp with a high coil resistance. However, this study will show that this minimum NF solution applies only if there is no damping resistor. The reason is that another factor related to the seismometer properties is involved when a damping resistor is present, as is usually the case.

It will also be shown that there is an optimum dependence of R_n on frequency and that this is best realized with FET-based op-amps or amplifiers with FET-like properties. Finally, by comparing the SNR's of three amplifier circuits, it is found that a parallel damping resistor with the noninverting op-amp circuits yields the best SNR.

All of the analysis that follows assumes system linearity, so that effects due to saturation and other nonlinear effects are not included. Also, effects due to cross-axis sensitivity, parametric effects (Rodgers, 1975), and suspension resonances are not considered.

THE SNR FOR AN EM SEISMOMETER

The objective is to find the optimum coil resistance, $r_{c,opt}$, that maximizes the SNR of an EM seismometer. A detailed derivation of a generalized model for the signal-to-noise ratio (SNR) referred to the coil terminals of an EM seismometer/preamplifier combination is given by Rodgers (1992) in which it is shown that the resulting model fit the experimental data closely. The model considers the four principal noise sources associated with an EM seismometer/preamplifier pair: the mechanical suspension noise, and the three electronic noises (Johnson noise, voltage noise, and current noise). This model is repeated in equation (1) below in slightly different form by the substitutions $\omega = 2\pi f$ and $\Omega = 2\pi f_o$:

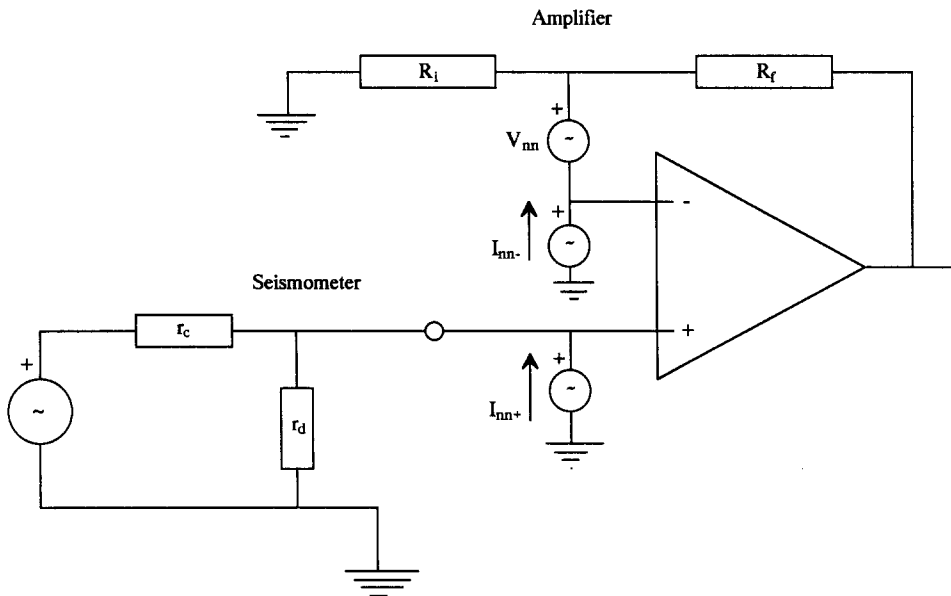
$$\text{SNR} = \frac{\left(\frac{r_d}{r_c + r_d} G \right)^2 \frac{4\pi^2 f^2}{(16\pi^4)(f_o^2 - f^2)^2 + 64\pi^4 \zeta^2 f_o^2 f^2} P_{aa}}{E_{nn} + \left(\left[\frac{r_d}{r_c + r_d} G \right]^2 \frac{4\pi^2 f^2}{[16\pi^4][f_o^2 - f^2]^2 + 64\pi^4 \zeta^2 f_o^2 f^2} \right) S_{nn}}. \quad (1)$$

P_{aa} is the acceleration power density spectra (acceleration pds) of the input acceleration, E_{nn} is the generalized pds of the total electronic noise associated with the seismometer and preamplifier, and S_{nn} is the pds of the suspension noise from the seismometer. The SNR given in equation (1) applies to the circuit shown in Figure 1; however, the derivation and exact form for E_{nm} for the three different op-amp configurations shown in Figure 10 are given in Rodgers (1992, Appendix A). The other terms in equation (1) are defined as follows: f = frequency in Hz, r_d = damping resistor in ohms, r_c = coil resistance in ohms, G = generator constant (open circuit) in V/m/sec, f_o = resonant frequency of the spring-mass systems, ζ = damping ratio.

The expression for the SNR given in equation (1) is based on using a damping resistor in parallel with the seismometer together with a preamplifier employing an operational amplifier in the non-inverting configuration. It will be shown later that this configuration, which is shown in Figure 1, results in a larger SNR than the other configurations. For this reason, it will be used in most of the subsequent development.

The Suspension Noise, S_{nn}

The suspension noise of a spring-mass system is due to the Brownian motion of its mass. The acceleration pds of the suspension noise, S_{nn} , is given by



*E-M Seismometer with Non-Inverting Amplifier
(Parallel Damping Resistor)*

FIG. 1. The noninverting amplifier configuration is shown. All the variables are pds's in V^2/Hz or A^2/Hz . V_{nn} , I_{nn-} , and I_{nn+} are the voltage noise and current noise pds's appearing at the terminals of the operational amplifier. The gain setting resistors are R_i and R_f , which produce a gain of $(1 + R_f/R_i)$. With I_{nn+} and I_{nn-} equal and only moderate gain, the source resistance for this configuration is given by the series combination of r_c in parallel with r_d and R_i in parallel with R_f . This shows why making R_i and R_f as small as the current limits of the op-amp permit results in the lowest noise.

equation (2), which can be derived from the expression given by Aki and Richards (1980) by substituting $\omega_s = 2\pi f_o$, and $Q = 1/2\zeta$:

$$S_{nn} = 16\pi \frac{kT\zeta f_o}{M}, \quad (\text{m/s}^2)^2/\text{Hz}. \quad (2)$$

where S_{nn} = suspension noise acceleration pds, $(\text{m/sec}^2)^2/\text{Hz}$; k = Boltzmann's constant = 1.38×10^{-23} Joules/ $^\circ\text{K}$; ζ = damping ratio of spring-mass system; M = mass; T = room temperature in $^\circ\text{K}$ = 293°K ; f_o = resonant frequency of the spring-mass system (Hz).

Total Electronic Noise Model

The total electronic noise, E_{nn} , appearing at the coil terminals of an EM seismometer connected to an op-amp-based preamplifier is given by equation (3). In Rodgers (1992, Appendix A), it is further shown that this equation is valid for both the inverting and noninverting op-amp configurations when the gain is at least moderately greater than unity.

$$E_{nn} = V_{oo} \left(\frac{f_{cv}}{f} + 1 \right) + I_{oo} \left(\frac{f_{ci}}{f} + 1 \right) R^2 + 4kTR, \quad (\text{V}^2/\text{Hz}), \quad (3)$$

where E_{nn} = total electronic noise voltage pds appearing at the input to the preamplifier (the coil terminals) in V^2/Hz ; $V_{oo}(\frac{f_{cv}}{f} + 1)$ = voltage noise pds, V_{nn} , at the inverting terminal in V^2/Hz (V_{oo} is the level at high frequencies and f_{cv} is the corner frequency); $I_{oo}(\frac{f_{ci}}{f} + 1)$ = noise current pds, I_{nn} , in A^2/Hz for noise current flowing from the inverting terminal (I_{oo} is the level at high frequencies and f_{ci} is the corner frequency; it is assumed that the noise current flowing from the noninverting terminal is identical); R = input or source resistance in ohms (for the inverting configurations, R is the total input resistance; for the noninverting configuration, R is the source resistance in series with the parallel combination of the gain setting resistances; Rodgers (1992, Part 1, Appendix A); $4kTR$ = Johnson or thermal noise, J_{nn} , generated due to the resistances in the circuit (the Johnson noise is different for the inverting and noninverting configurations; the exact expressions for each are given in Rodgers (1992, Appendix A)).

In the inverting configuration no noise current flows through the input resistance, R , (Riedesel *et al.*, 1990). Nevertheless, because of the gain action of the op-amp, I_{nn} is multiplied by a gain term resulting in the expression $I_{nn}R^2$ in E_{nn} in equation (3) (Rodgers, 1992, Appendix A). It will be seen later that this term has a major effect on the SNR of the seismometer and preamplifier combination.

The three circuits considered in this paper are all single-ended for simplicity. Because of the need for common mode rejection, most seismic data recorders use differential (double-ended) input circuits. Usually these differential circuits consist of three op-amps with two in front in the noninverting configuration with a single differential summing amplifier in back to difference the two signals. The seismometer is connected between the two noninverting inputs.

This arrangement doubles E_{nn} and I_{nn} but not the Johnson noise, J_{nn} . Therefore, the total electronic noise for the differential input amplifier is slightly less than twice the noise for the single-ended input. It will be seen later that doubling both E_{nn} and I_{nn} produces no change in R_n . Therefore, R_n is the same for single-ended and differential configurations.

The amplifier noise parameters are given for six op-amps in Table 1. However only three of them are used in the numerical examples to follow because the LT1012, LT1079, and AD743 all have R_n 's too large to be compatible with most coil resistances. The location of these noise sources in the amplifier configuration being studied is shown in Figure 1. The voltage source is shown in series and the two current sources in parallel (Tobey *et al.*, 1971). The details of exactly how these noise sources appear in the amplifier output are given in Rodgers (1992, Appendix A). As can be seen from the first two terms in equation (3), both V_{nn} and I_{nn} rise with a -1 slope as frequency decreases. This is due to the flicker of $1/f$ noise (Horowitz and Hill, 1989) and is the factor that causes the SNR to decrease with decreasing frequency. The parameters V_{oo} , f_{cv} , I_{oo} , and f_{ci} are given in Table 1 for the four representative low-noise op-amps used in this study.

The circuit configuration from which equation (1) was developed is shown in Figure 1. The damping resistor, r_c , is in parallel with the seismometer terminals, and the op-amp is connected in the noninverting configuration. The two gain setting resistors, R_i and R_f , determine the gain for this configuration which is $1 + (R_f/R_i)$. The voltage noise source, V_{nn} , and the two current noise sources, I_{nn-} and I_{nn+} , discussed in the previous section are indicated.

As detailed in Rodgers (1992, Appendix A), for this noninverting configuration, the source resistance, R , is given by

$$R = \frac{r_c r_d}{r_c + r_d} + \frac{R_f R_i}{R_f + R_i} \quad (\text{ohms}). \quad (4)$$

The reason for using the noninverting, parallel damping resistor configuration now becomes apparent. It allows the gain setting resistors to be set independently without loading the seismometer. In order to maximize the SNR, it is

TABLE 1
NOISE PARAMETERS FOR SIX OPERATIONAL AMPLIFIERS

Operational Amplifier	V_{oo} (V ² /Hz)	f_{cv} (Hz)	I_{oo} (A ² /Hz)	f_{ci} (Hz)	R_o (ohms)
Linear Technology, LT1028	7.2×10^{-19}	3.5	8.1×10^{-25}	250	943
Linear Technology, LT1012	1.9×10^{-16}	2.5	3.6×10^{-29}	120	2.3 M
Linear Technology, LT1079	7.8×10^{-16}	0.7	4.0×10^{-28}	200	1.4 M
Analog Devices, AD743	9.00×10^{-18}	30	6.4×10^{-29}	140	3.75 K
Precision Monolithics, OP-27	9.0×10^{-18}	2.7	1.6×10^{-25}	140	7500
Precision Monolithics, MAT-02					
At $I_c = 60 \mu\text{A}$	1.36×10^{-17}	8	2.5×10^{-25}	8	7400
At $I_c = 100 \mu\text{A}$	6.2×10^{-18}	8	6.4×10^{-25}	8	3000

Note: R_o is the level of the noise resistance at high frequencies ($f \gg f_{ci}$) and is given by $R_o = \sqrt{\frac{V_{oo}}{I_{oo}}}$.

desirable to minimize the source resistance, R , so R_i and R_f are to have as low values as possible. In this study, the limiting case will be considered in which the gain setting resistors are chosen so low that their parallel combination is much less than the parallel combination of r_d and r_c . Usually this means that $R_i \ll r_c$. Of course, because of current limitations in the op-amp, it may not be possible to realize this in practice, particularly for seismometers with low coil resistances. However, because of the trend toward using seismometers with larger coil resistances, the requirement can be at least approximated. In any event, it serves as a useful limiting case. Based on these considerations, the source resistance, R , will be replaced by r_p , where

$$r_p = \frac{r_c r_d}{r_c + r_d} \quad (\text{ohms}). \quad (5)$$

With this change, R is set equal to r_p in equation (3), resulting in the expression for E_{nn} given in equation (6):

$$E_{nn} = V_{oo} \left(\frac{f_{cv}}{f} + 1 \right) + I_{oo} \left(\frac{f_{ci}}{f} + 1 \right) r_p^2 + 4kTr_p \quad (\text{V}^2/\text{Hz}). \quad (6)$$

MAXIMIZING THE SNR WITH RESPECT TO COIL RESISTANCE

In order to proceed with finding $r_{c,opt}$, which is the value of r_c that maximizes the SNR, the functional dependence on r_c of several terms in equation (1) must be specified.

E_{nn} in equation (6) is dependent on r_p , which, in turn, is dependent on r_c through the parallel resistance formula given by equation (5). The unloaded generator constant, G , depends on r_c via the relationship (Riedesel *et al.*, 1990, Appendix 1)

$$G = C\sqrt{r_c} \quad (\text{V/m/sec}). \quad (7)$$

For a given seismometer, C is nearly constant regardless of the coil resistance because the coil volume (bobbin size) and magnetic field remain nearly constant. Values for the parameter C for nine EM seismometers are given in the next to last column in Table 2. For a selected damping ratio, ζ , the damping resistor, r_d , depends on all the other seismometer parameters. The relationship is given by equation (8), which is derived in Appendix A:

$$r_d = \left(\frac{C^2}{4\pi M f_o (\zeta - \zeta_o)} - 1 \right) \cdot r_c \quad (\text{ohms}). \quad (8)$$

In equation (8), ζ_o is the open-circuit damping ratio of the seismometer. When there is no damping resistor present, the only damping is the open-circuit damping, which is to say that $\zeta = \zeta_o$. The result is that r_d goes to infinity, which is the proper result since it is in parallel with the seismometer. The suspension noise, S_{nn} , given by equation (4) is not a function of r_c since ζ is a constant specified by the user or set by the manufacturer, just as are the resonant frequency, f_o , and the mass, M .

TABLE 2
INSTRUMENTAL PARAMETERS FOR NINE EM SEISMOMETERS

Seismometer Type	$f_o = F$ (Hz)	G (V/m/sec)	ζ	ζ_0	M (Kg)	r_c (ohms)	r_d (ohms)	C (V-s/m-ohms ^{1/2})	SF
Oyo-Geospace HS-1	4.5	62.2	0.6	0.3	0.0227	2500	7500	1.24	1.33
Mark Products L-22D	2.0	112.0	0.8	0.46	0.0728	5470	14300	1.49	1.78
Sprengnether S-6000CD	2.0	373.3	0.6	0.35	0.5	10000	11000	3.73	2.42
Mark Products L-4C	1.0	276.4	0.7	0.46	1.0	5500	8900	3.73	2.87
Kinemetrics SS-1	1.0	345.0	1.0	0.05	1.45	5000	6530	4.879	3.66
Teledyne-Geotech S-13	1.0	629.0	1	0.053	5.0	3600	6300	10.483	2.18
Teledyne-Geotech GS-13	1.0	2150	1	0.02	5.0	8900	74500	22.8	1.13
Kinemetrics SV-1	0.2	270	1	0.043	1.0	3800	22000	4.38	1.14
Teledyne-Geotech SL-210V, SL-220H	0.05	90	1	0.05	2.0	1200	6440	2.60	1.22

Notes: ζ , ζ_0 , and SF are all dimensionless ratios. The parameters of the Kinemetrics SH-1 are the same as those for the SV-1 except that $\zeta_0 = 0.026$.

To summarize, in the numerator of the SNR, r_c appears to the first power in both G^2 and in the numerator and denominator of the voltage divider fraction that precedes it. In the denominator of the SNR, it appears in the same way in the fraction preceding S_{nn} . Also, in the denominator it appears in E_{nn} to the first power and squared through r_p , which has r_c in both its numerator and denominator. The result is that the SNR is seen to be a complicated function of the coil resistance, r_c , and the frequency, f . Because of this analytical complexity, it is useful to examine a plot of the function SNR (r_c, f).

In order to plot the SNR, numerical values must be chosen for the various parameters in the expression. This requires selecting a particular seismometer-amplifier pair and an input acceleration pds, P_{aa} . For this plot, the frequently used combination of the 1-Hz Mark Products L-4C seismometer paired with the Precision Monolithics, Inc. (PMI), OP-27 op-amp has been selected. The parameters for the noise model for the OP-27 in the first two terms of equation (3) are given in Table 1. In order to have an SNR larger than one for all the seismometers, the input acceleration selected is the constant high frequency (> 1 Hz) level of Peterson's high noise model (HNM) (Peterson, private comm., 1991). This results in

$$P_{aa} = 7.8 \times 10^{-15} \quad \left((\text{m/sec}^2)^2 / \text{Hz} \right). \quad (9)$$

For perspective, this can be compared with Peterson's low noise model (LNM) (Peterson, 1982; Peterson and Hutt, 1982; Peterson and Tilgner, 1985; Peterson and Hutt, 1989), in which the level above 1 Hz is $1.6 \times 10^{-17} (\text{m/sec}^2)^2 / \text{Hz}$.

Because P_{aa} is a constant for all frequencies in this study, the resulting SNR's as a function of frequency are not meant to define the useful lower limit of the seismometer-amplifier pairs as they do in Rodgers (1992). An analytical advantage of using a constant acceleration pds input is that it guarantees that the maximum SNR as a function of r_c corresponds to a minimum in the noise at that same value. This is not necessarily the case when the actual HNM or LNM is used since then the location of the maximum of the SNR also depends on the input acceleration pds.

Based on these considerations, a 3D plot of the SNR (r_c, f) is shown in Figure 2 for the L-4C seismometer and OP-27 op-amp combination. The f axis is the hidden axis going into the page and the r_c axis is the one coming out of the page from left to right. For every value of r_c , the SNR has a sharp maximum as a function of f . This is to be expected as shown in Rodgers (1992). However, the interesting feature of Figure 2 is that for each value of f the SNR also has a maximum as a function of r_c . In order to see this more clearly, a slice is taken through the curve at $f = 1$ Hz. This is shown in Figure 3, which clearly shows the maximum. The value of r_c for which the SNR is a maximum is labeled $r_{c,opt}$. It is clear that coil resistances larger than $r_{c,opt}$ result in some reduction in the SNR but that coil resistances less than the optimum can produce severe degradation in the SNR. Numerical examples of this will be shown later.

The optimum coil resistance, $r_{c,opt}$, is now found from

$$\frac{\partial \text{SNR}(r_c, f)}{\partial r_c} = 0. \quad (10)$$

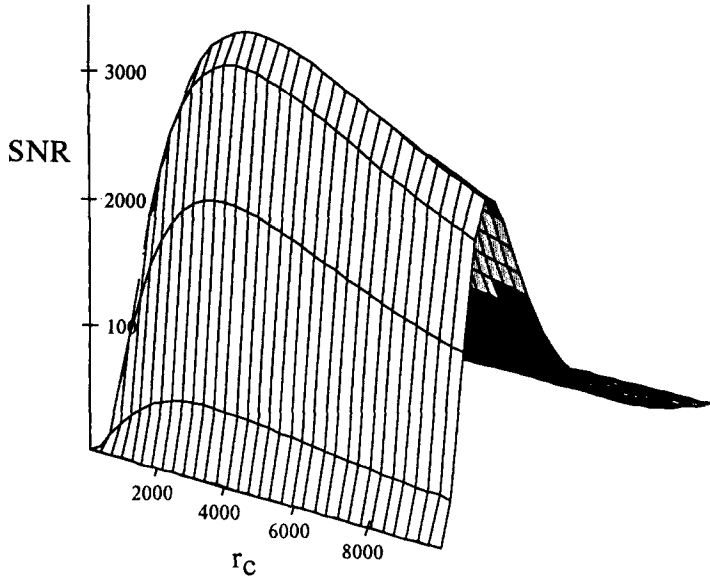


FIG. 2. A three-dimensional plot of the function $\text{SNR}(r_c, f)$ is shown. The hidden axis going into the page is the frequency axis, f . The coil resistance axis, r_c , is the exposed axis coming out of the page. The seismometer-amplifier pair used for this plot are the Mark Products 1-Hz L4-C seismometer and the Precision Monolithics, Inc., OP-27 op-amp. The SNR has a maximum as a function of r_c , so it is apparent that there is an optimum coil resistance for the seismometer-amplifier pair.

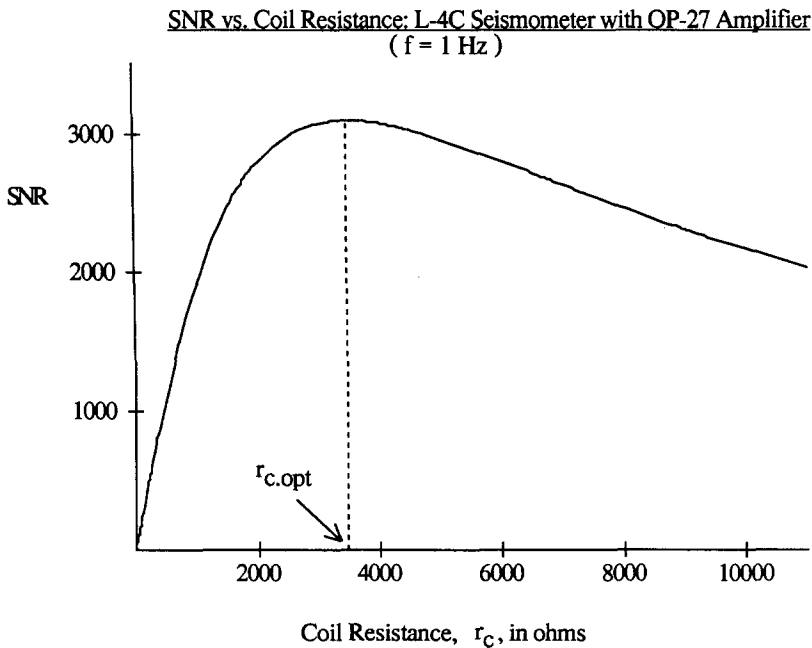


FIG. 3. This figure is a plot of the function $\text{SNR}(r_c, 1)$, which is a slice through the three-dimensional plot of Figure 2 at $f = 1 \text{ Hz}$. The coil resistance, r_c , that maximizes the SNR is indicated on the horizontal axis as $r_{c,\text{opt}}$. The seismometer-amplifier pair used are the L-4C seismometer and the OP-27 op-amp.

It is surprising that, despite the complicated analytic dependence of the SNR on r_c , the result is a simple analytical expression for $r_{c.opt}$, which is given in equation (11):

$$r_{c.opt} = \left(\frac{1}{1 - \frac{4\pi M f_o (\zeta - \zeta_o)}{C^2}} \right) \times \left(\frac{V_{nn}}{I_{nn}} \right)^{\frac{1}{2}} \quad (\text{ohms}). \quad (11)$$

Seismometer Factor Noise Resistance

The function $r_{c.opt}$ is composed of two factors. The first, called the seismometer factor (SF), is a dimensionless constant involving all the seismometer parameters. Computed SF's for nine EM seismometers are given in the far right hand column of Table 2. It would be useful if seismometer manufacturers would include SF's with their other specifications. The second factor in equation (11) is a function of the noise properties of the op-amp and is termed the noise resistance, R_n . It is defined (Horowitz and Hill, 1989) as

$$R_n = \sqrt{\frac{V_{nn}}{I_{nn}}} \quad (\text{ohms}). \quad (12)$$

R_n is frequency dependent through V_{nn} and I_{nn} , which are functions of frequency as indicated by the first two terms in equation (3). For the four representative amplifiers used in this study, the parameters necessary for computing R_n are given in Table 1. Plots of R_n versus frequency are shown in Figure 4 for the three frequently used low-noise op-amps: the PMI OP-27 and MAT-02, and the Linear Technology Corporation LT1028. The R_n 's of the two bipolar based op-amps, the LT1028 and the OP-27, vary considerably with frequency. For these two much-used op-amps, it is unfortunate that R_n is so frequency dependent because, of course, seismometer coil resistances are constants independent of frequency, and it is desirable to have the optimum coil resistance track the actual coil resistance over as great a frequency range as possible. The consequences of the frequency dependence of R_n for these two op-amps will be seen in the numerical examples to follow. The R_n properties of the FET-based Analog Devices AD743 and the FET-like MAT-02 will be discussed later. The AD743 was not included in Figure 4 because its R_n is too large, approximately 375 k-ohms, to be compatible with most seismometer coil resistances.

In summary, to obtain the optimum coil resistance, multiply the SF of the seismometer by the R_n of the op-amp as indicated in equation (13).

$$r_{c.opt} = \text{SF} \times R_n \quad (\text{ohms}). \quad (13)$$

Relationship to the Minimum Noise Figure Result

The noise figure (NF) of an amplifier is defined (Horowitz and Hill, 1989)

$$\text{NF} = 10 \log_{10} \left(\frac{V_{nn} + I_{nn} R^2 + 4kTR}{4kTR} \right), \quad (14)$$

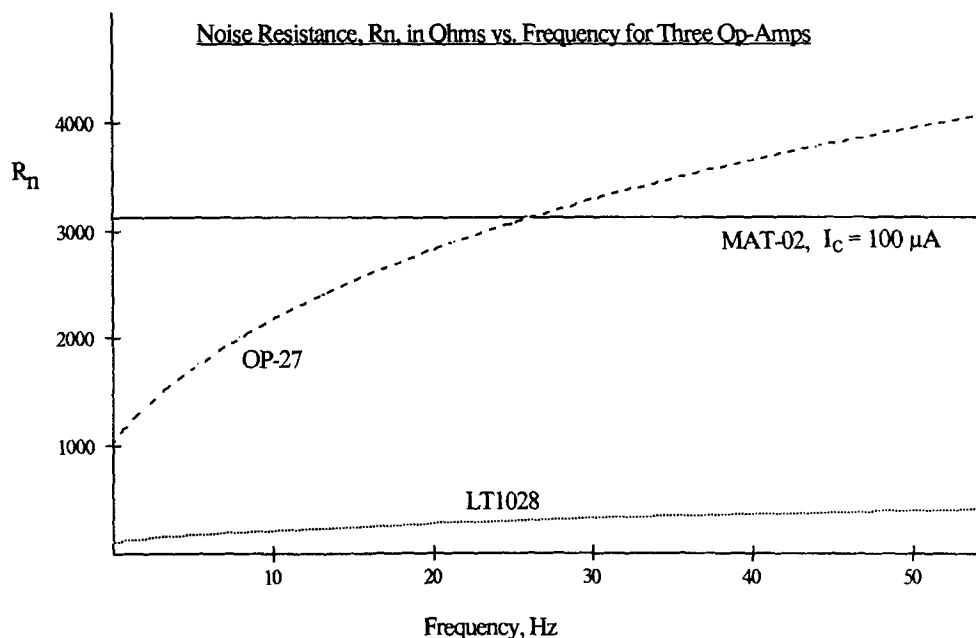


FIG. 4. This figure plots the R_n , as a function of frequency for the LT1028, OP-27, and MAT-02 (for $I_c = 100 \mu\text{A}$) op-amps. The curves were generated using the op-amp data from Table 1. It is seen that the LT1028 has a very low R_n , whereas the OP-27 and MAT-02 exhibit larger values. The MAT-02 has the desirable characteristic that its R_n is a constant independent of frequency.

where R is the source resistance. In physical terms, this is the ratio (in dB) of the noise referred to the input of an actual amplifier to that of an ideal noise free amplifier whose only noise is the irreducible Johnson noise from the source resistance, R . The expression for R that minimizes the NF is termed the noise resistance, R_n , and is defined by the previously given equation (12).

The relationship between the minimum NF solution and the solution in this study for the optimum coil resistance can be seen by setting $\zeta = \zeta_o$ in the expression for $r_{c,opt}$, equation (11). Physically this corresponds to removing the damping resistor, r_d , so that the only damping present is the open circuit damping, ζ_o . For $\zeta = \zeta_o$, the SF becomes unity, and $r_{c,opt}$ reduces to the minimum NF solution as shown in equation (15):

$$r_{c,opt} = \left(\frac{V_{nn}}{I_{nn}} \right)^{\frac{1}{2}} = R_n. \quad (15)$$

This demonstrates that the minimum NF solution is a special case of equation (11) where there is no damping resistor. The correspondence between the two solutions is reasonable because removing the damping resistor means that the source resistance, R , in the minimum NF solution is just the coil resistance of the seismometer, r_c . Another interesting point is that the expression given in equation (11) is bilateral; given a coil resistance, equation (11) can be used to find the optimum R_n .

To summarize, if the seismometer is damped by a fluid or by eddy currents so that no damping resistor is present, the optimum coil resistance is given by the R_n however, if, as is usually the case, the seismometer is damped by using a damping resistor, the optimum coil resistance is obtained by multiplying the SF by the R_n as shown in equation (13).

NUMERICAL EXAMPLES

The following sets of examples illustrate selecting a coil resistance based on a computed $r_{c.opt}$ and the effect of the choices made on the resulting SNR's. In addition, they will show the effect of selecting different op-amps with the same seismometer. Finally, the performance of the three commonly used op-amp circuits will be compared.

Amplitude Signal-to-Noise Ratio (ASNR)

The SNR is defined as a ratio of powers and so is not always convenient in seismology, where most of the work is carried on in terms of amplitudes. Therefore, to make the following numerical examples more meaningful, the results will be given in terms of the amplitude signal-to-noise ratio (ASNR) instead of the SNR. The ASNR is defined as:

$$\text{ASNR} = \frac{\text{Signal Amplitude}}{\text{Noise Amplitude}}. \quad (16)$$

In this study, these amplitudes are amplitude density spectra (ads), which are the square root of the power density spectra (pds) used earlier. Therefore the ASNR can be written as

$$\text{ASNR} = \frac{\sqrt{P_{ss}}}{\sqrt{P_{nn}}}. \quad (17)$$

Comparing this form for the ASNR with the definition of the SNR shows that the ASNR is obtained from the SNR by

$$\text{ASNR} = \sqrt{\text{SNR}}. \quad (18)$$

Of course, in terms of dB the two are equal.

The L-4C Seismometer with the OP-27 Op-Amp

The standard Mark Products 1 Hz L-4C seismometer is available with coil resistances of 500, 2000, and 5500 ohms. This example will compare the ASNRs of the 5500- and 500-ohm versions with different op-amps.

From Table 2, the dimensionless SF of the L-4C is 2.87. This is independent of the coil resistance. Assume that the 5500-ohm coil resistance is chosen and that it is desired to select an op-amp to go with it for the maximum ASNR. The scheme is to select an op-amp such that $r_{c.opt} = r_c$ as nearly as possible over the

frequency range of interest. Therefore, choose an op-amp having an R_n such that over the frequency range of interest, as nearly as possible:

$$R_n \approx \frac{r_c}{SF}. \quad (19)$$

The quotient $5500/2.87$ is approximately 2000 ohms. Entering the R_n axis of Figure 4 with this value shows that the OP-27 would be a good choice, with a close match at approximately 8 Hz. Using equation (11), $r_{c,opt}$ is plotted versus frequency in Figure 5 for the L-4C with the OP-27 op-amp. The 5500-ohm coil resistance is also shown to indicate the frequency range over which they are reasonably equal. The resulting ASNR will be displayed in a subsequent figure.

For comparison purposes, assume instead that the 500-ohm coil resistance is selected. Dividing 500 by 2.87 results in approximately 180 ohms, so it appears that the LT1028 would be the only candidate. The resulting $r_{c,opt}$ versus frequency for the L-4C with the LT1028 is shown in Figure 6. From both Figures 5 and 6, it would appear that a large ASNR would be expected only at low frequencies. This is confirmed by Figure 7, which compares the ASNR's that result from each coil resistance op-amp pair. The resulting ASNR's for each pair are nearly identical. Figure 7 also shows that the ASNR degrades badly outside the frequency band of 1 to 4 Hz because of the frequency dependence of $r_{c,opt}$. This is rather disappointing and indicates that this is an area that needs attention.

Finally, the point should be made that having a large ASNR does not mean that there is also a large signal. Certainly the signal with the 5500-ohm coil will

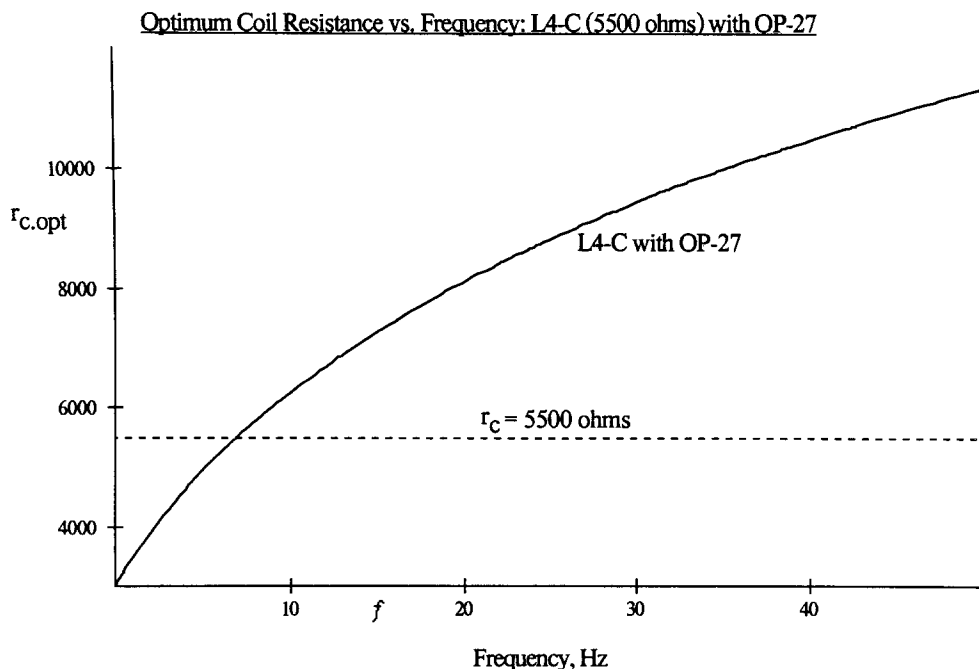


FIG. 5. The optimum coil resistance, $r_{c,opt}$, is shown versus frequency for the 1-Hz L-4C (5500 ohms) seismometer with the OP-27 op-amp used as a preamplifier. The coil resistance for this seismometer is plotted as the horizontal dashed line. Because of the frequency dependence of the R_n of the OP-27, $r_{c,opt}$ is equal to the 5500-ohm coil resistance only near 8 Hz.

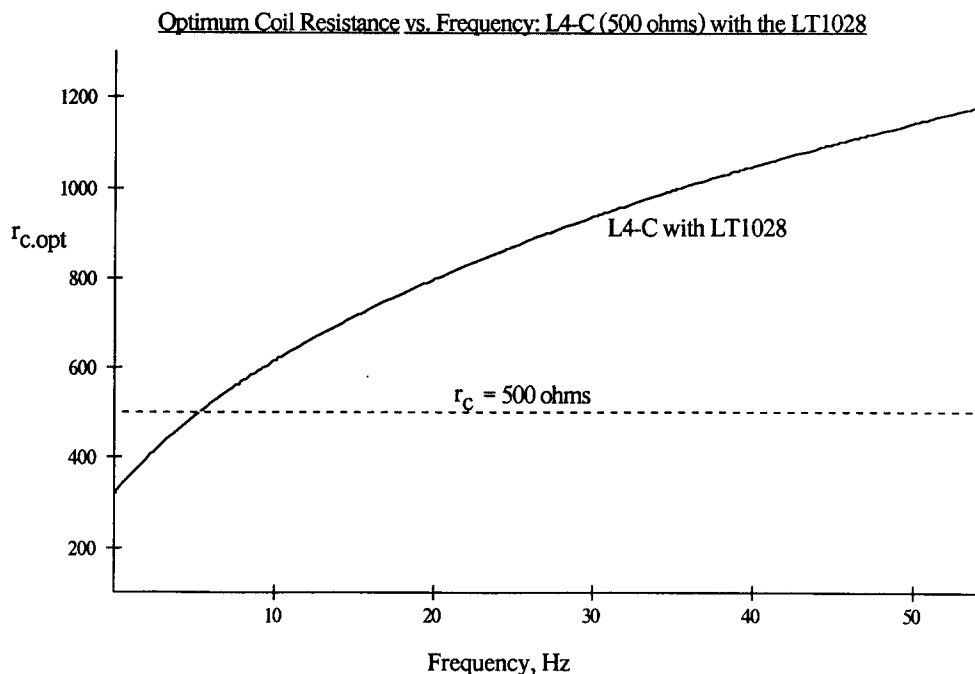


FIG. 6. The optimum coil resistance, $r_{c.opt}$, is shown versus frequency for the 1-Hz L-4C (500-ohm) seismometer with the LT1028 op-amp used as a preamplifier. The coil resistance for this seismometer is plotted as the horizontal dashed line. Because of the frequency dependence of the R_n of the LT1028, $r_{c.opt}$ is equal to the 500-ohm coil resistance only near 5 Hz.

be about 3 times that from the 500 ohm coil. For approximately equal ASNR's, as in this case, the correct policy is to choose the larger coil resistance in order to maximize the signal and, therefore, minimize the amount of electronic gain required following the seismometer. Furthermore, if the coil resistance is not the optimum value, it is seen from Figure 5 that the resulting decrease in the ASNR is less if the coil resistance is chosen to be greater than the optimum value rather than less.

The Effect of Amplifier Type on the ASNR: The GS-13 with Three Different Op-Amps

In the previous example, care was taken to match the coil resistance and op-amp to maximize the ASNR. The question then arises regarding how deleterious it is when they mismatched. The comment might be made that one would never do this, but, unfortunately, it could happen when an EM seismometer is connected to a seismic recorder. Certainly the type of op-amp, together with its R_n characteristics, used in the input stage of a seismic recorder is information not generally available from manufacturers. It will be seen later that even the type of circuit used makes a significant difference. It is hoped that this study will motivate the manufacturers of seismic recorders to make this type of information more available.

In this example, for comparison purposes, the nominally 1-Hz Teledyne Geotech GS-13 seismometer is paired with three different op-amps: the LT1028, the OP-27, and the MAT-02. Some explanation regarding the MAT-02 is neces-

Comparison ASNR's for Two L-4C Configurations: the 500 ohm coil with the LT1028 and the 5500 ohm coil with the OP-27

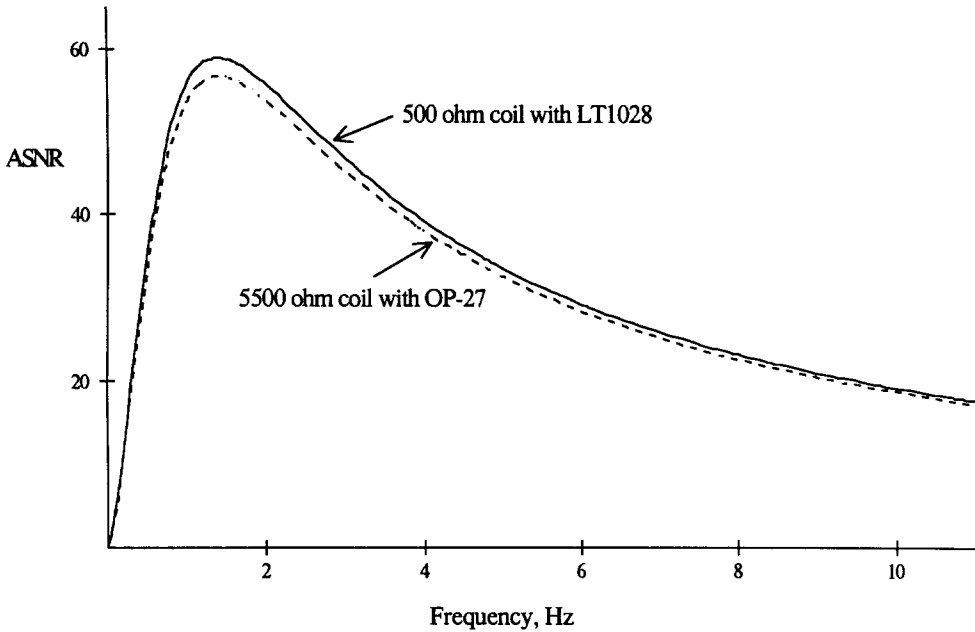


FIG. 7. The ASNRs are compared for two L-4C pairings: the 5500-ohm L-4C with the OP-27 op-amp, and the 500-ohm L-4C with the LT1028 op-amp. The resulting ASNRs are nearly identical. This does not mean, however, that the signals are equal, because the 5500-ohm unit will always have about 3 times the signal of the 500-ohm unit. Given equal ASNRs for two combinations, it is always best to use the seismometer having the largest generator constant.

sary. The MAT-02 is a FET-like dual monolithic transistor whose R_n can be adjusted over a considerable range by adjusting its collector current, I_c . With a collector current of 1 mA, the R_n drops to around 1 K-ohm. At the other extreme, a collector current of 1 μ A results in an R_n of 400 K-ohms. Since the manufacturer's literature is difficult to interpret, these values must be regarded as approximate. Even more approximate are the values used here for the voltage and current pds's corner frequencies, f_{cv} and f_{ci} . To the author, they appear to be equal. As will be seen, this results in an R_n independent of frequency, which was shown in the last section to be a very desirable characteristic. This almost constant R_n characteristic also appears in the FET-based AD743 op-amp mentioned earlier. The R_n of the AD743 actually decreases slightly with frequency. A disadvantage of the MAT-02 is that it is only a matched transistor pair and thus must be combined with an op-amp, with the MAT-02 serving as the differential first stage. The feedback resistance, R_f , then goes around the cascaded pair. Obviously, more investigation of the MAT-02 and other amplifiers with adjustable and nearly constant noise resistance is in order.

The GS-13 has a coil resistance of 8900 ohms and (from Table 2) an SF of only 1.135. From equation (19), to match $r_{c,opt}$ an R_n of $8900/1.135$ or 7800 ohms is required. This is nearly achieved by the MAT-02 with a collector current, I_c , of 60 μ A, which results in $R_n = 7400$ ohms. Using the above data, Figure 8 plots $r_{c,opt}$ versus frequency for the GS-13 matched with the MAT-02 and

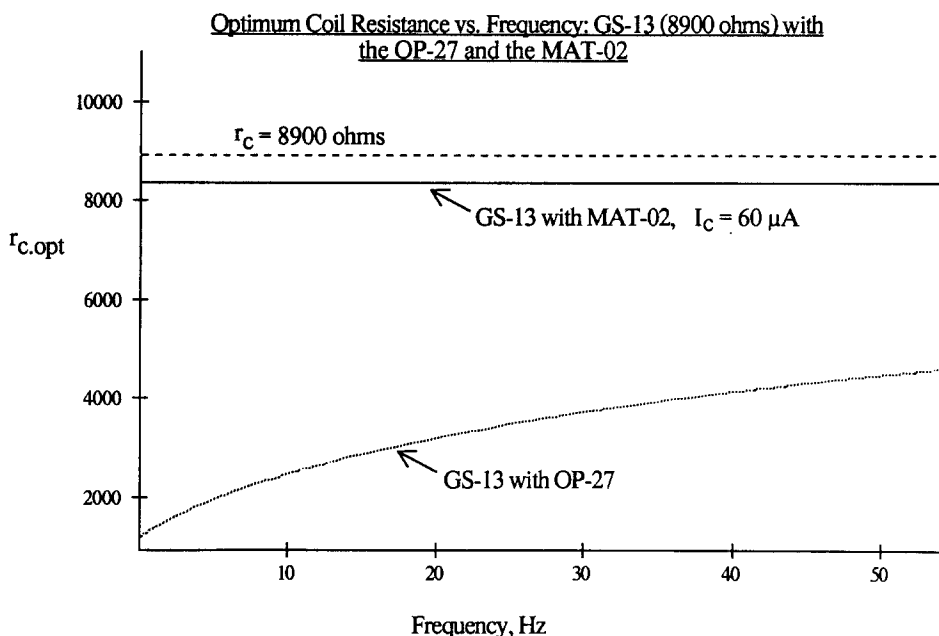


FIG. 8. This figure compares the optimum coil resistance, $r_{c,opt}$, versus frequency for the GS-13 seismometer paired with three op-amps: the OP-27, the MAT-02 ($I_c = 60 \mu A$), and the LT1028, which does not appear in this plot but does on Figure 9. The 8900-ohm coil resistance of the GS-13 is shown as a dotted line. It is seen that the OP-27 is clearly a much poorer match for the GS-13 than the MAT-02. The results of the mismatch are shown in Figure 9.

mismatched with the LT1028 and OP-27, both of which have much too low an R_n . The curve for the LT1028 is too low to appear on this graph. The $r_{c,opt}$ using the OP-27 rises from about 1000 ohms at 0 Hz to about 5000 ohms at 50 Hz. This is well below the 8900-ohm coil resistance of the GS-13 shown as the dashed line.

To demonstrate the deleterious effect on the ASNR of mismatching seismometer and op-amp, Figure 9 plots the resulting ASNRs for each case. Obviously the match with the MAT-02 is better, but the OP-27 is only worse by approximately one third, with an average mismatch of about 6 K-ohms. The mismatch with the low R_n LT1028 results in a more than 200% degradation in the ASNR. A user would not knowingly implement such a mismatch of seismometer and amplifier, but it could happen inadvertently when connecting the GS-13 or other EM seismometer to a seismic recorder whose preamplifier noise resistance characteristics are unknown to the user; this unfortunately is usually the case. Manufacturers of seismic recorders are urged to supply information on the R_n of the analog front end of their recorders when it is available from the manufacturer of the op-amp being used.

The op-amp manufacturer's specifications often give the voltage noise pds, $V_{nn}(f)$, but not the current noise pds, $I_{nn}(f)$. So $R_n(f)$, is not known for these op-amps. An example is the PMI AMP-01. On the other hand, the often used PMI OP-270 has noise properties similar to the OP-27. As discussed earlier, the differential configuration has twice the voltage noise, E_{nn} , and current noise, I_{nn} , of the single-ended configuration. But it is seen from equation (12) that doubling both of these keeps R_n the same. Therefore, the R_n of the OP-270 is the same as that of the OP-27 given in Figure 4. The R_n of the PMI OP-77 can

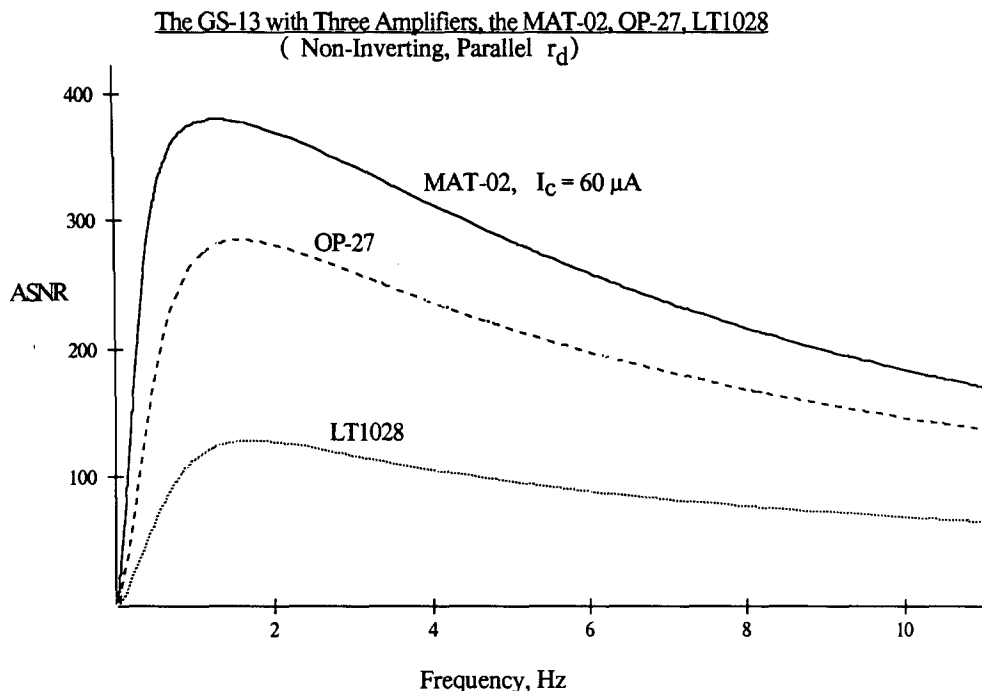


FIG. 9. The ASNRs resulting from pairing the GS-13 with the LT1028, OP-27, and the MAT-02 with $I_c = 60 \mu A$ are compared. The ASNR using the LT1028 is down a factor of about 3 compared to the MAT-02, and the OP-27 is down a factor of about 1.3. Such gross mismatching would not be purposely done but can accidentally occur when connecting an EM seismometer to a seismic recorder whose input R_n properties are unknown, as is generally the case.

be obtained from the manufacturers data on the total electronic noise by using equation (3) to obtain I_{nn} (O.D. Starkey, personal comm., 1992).

The Effect of Circuit Type on the ASNR

The purpose of this section is to compare the ASNRs of three types of single-ended op-amp circuits used with EM seismometers. These are shown in Figure 10. As in Figure 1, the locations of the various noise sources are shown. For both the inverting (top two) and noninverting (bottom) circuits, the details of the effects of these noise sources are given in Rodgers (1992, Appendix A).

The top circuit employs a damping resistor, r_d , in parallel with the seismometer (i.e., across the seismometer terminals) feeding into the standard noninverting op-amp configuration. In order to avoid loading down the damping resistor and thus increasing the seismometer damping, the input resistance, R_i , to the op-amp must be made larger than r_d , such as 5 to 10 times larger. The reason that R_i loads r_d is that its right-hand side is connected to the inverting terminal of the op-amp, which is very near ground potential (virtual ground). The undesirable effect of making R_i much larger than r_d is that it makes the source resistance, R , in equation (3) quite large. This results in a large value of the total electronic noise, E_{nn} , thus decreasing the ASNR. It will be seen in the next figure that this is the poorest of the three circuits.

The middle circuit takes advantage of the fact that the inverting terminal of the op-amp is at virtual ground by connecting r_d directly to it. The gain of this

Three Circuits for E-M Seismometers

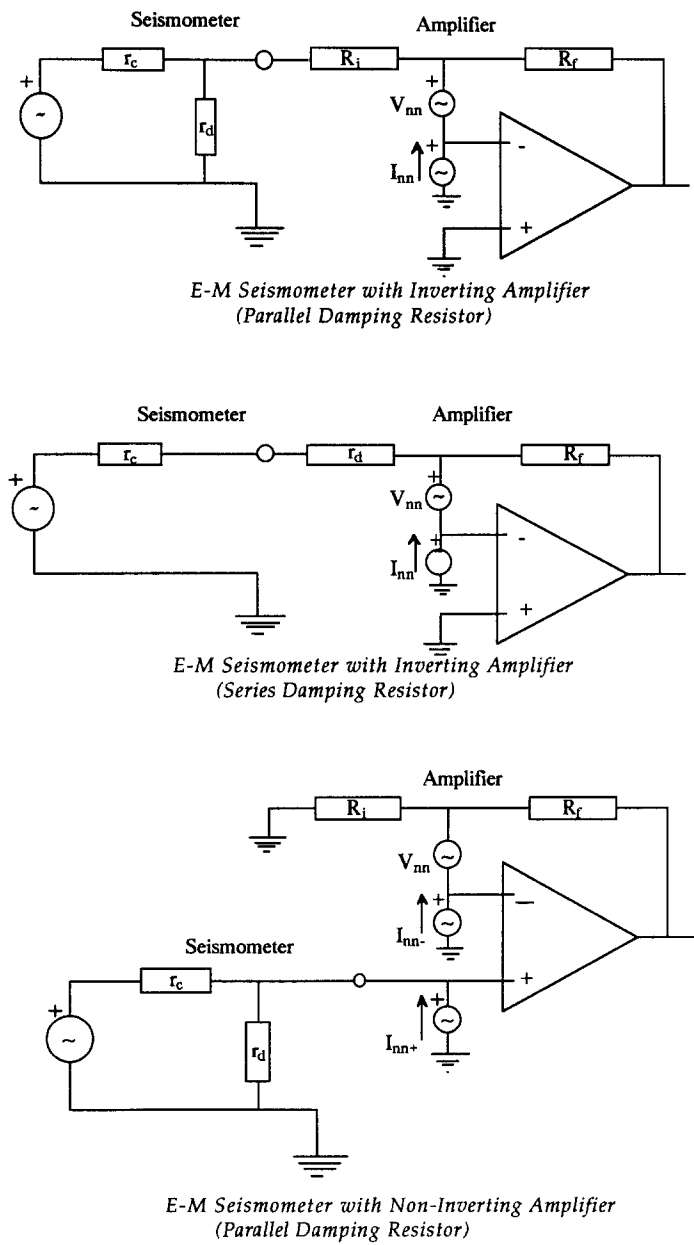


FIG. 10. The three commonly used single-ended op-amp circuits used as preamplifiers for EM seismometers are shown together with their noise sources. The top circuit uses a damping resistor in parallel with the seismometer feeding into an inverting op-amp configuration. In this circuit, $R_i \gg r_d$, to avoid loading r_d . This results in a very large source resistance, R , with the accompanying noise penalty. The middle circuit places the damping resistor in series with the coil resistance directly into the inverting op-amp. This also results in a large source resistance, R , when the damping resistance is large as they tend to be for modern large generator constant seismometers. In terms of noise, the preferred circuit is shown at the bottom, in which the damping resistor is in parallel with the coil resistance as in the top circuit. The advantage is that, in this noninverting configuration, R_i does not load r_d and so can be kept to a low value. Thus the noise penalty is less than that of the upper two circuits.

circuit from the seismometer terminals is then effectively $-R_f/r_d$. However, the problem with this configuration is that it puts the damping resistance, r_d , in series with the coil resistance, r_c . In modern EM seismometers having high generator constants, r_d can be as much as 9 times r_c ; so putting r_d and r_c in series results in a large value for the source resistance, R . Consequently, there is a degradation in the ASNR, although not as severe as that for the top circuit.

The bottom circuit is the same as that shown in Figure 1 and is repeated here for comparison with the other two circuits. It puts the damping resistor in parallel with the seismometer coil so that the source resistance through which I_{nn+} flows is r_d in parallel with r_c , which is less than r_c itself. The gain setting resistors, R_f and R_i , can, within limits, be kept low without loading down the damping resistor, which was the problem in the top circuit. The total source resistance, R , for this noninverting configuration was given previously by equation (4). It can be seen that the source resistance, R , for this circuit can be made considerably smaller than for the upper two circuits, so that an enhanced ASNR is to be expected. Although these considerations are for the three single-ended circuits, the same would apply to their differential (double-ended) equivalents.

In Figure 11, the ASNR's for the three circuits shown in Figure 10 are compared using the same seismometer/amplifier pair for each circuit. The pair used are the GS-13 with the MAT-02 with $I_c = 60 \mu\text{A}$. The lower, dotted curve is the ASNR for topmost circuit with the inverting amplifier and the parallel r_d . The dashed middle curve is the ASNR for the middle circuit, which also uses an inverting amplifier but with r_d in series. This configuration offers about a 50% improvement over the inverting, parallel r_d circuit. For the reasons stated earlier, the bottom circuit using the noninverting amplifier with r_d in parallel results in the largest ASNR by some 350%.

The GS-13/MAT-02 pair used in this example represent a worst case for the top two circuits because the GS-13 has such a large damping resistor, 74.5 K-ohms. So making R_i large enough not to load r_d in the inverting parallel r_d configuration or putting r_d in series with r_c in the inverting series r_d circuit both result in very large source resistances. Although this extreme case was chosen to emphasize the point about the optimum circuit, large damping resistances are becoming more common as increasingly "super" versions of seismometers become available such as the super L-22D ($r_d = 14$ K-ohms), and the "super" L-4C ($r_d = 55$ K-ohms).

CONCLUSIONS

This study begins by showing that for a given EM seismometer and preamplifier pair there is an optimum coil resistance that maximizes the SNR. This optimum coil resistance is a simple analytical expression given by the product of the SF of the seismometer and the R_n of the amplifier. In examining the optimum coil resistance, it is seen that an R_n independent of frequency is desired. It appears that FET-based or FET-like op-amps have this desirable characteristic; and at least one, the MAT-02, permits adjusting the level of its R_n by adjusting the collector current to satisfy equation (19).

The deleterious effects of mismatching seismometer and amplifier are shown by comparing ASNRs for the GS-13 seismometer paired with three different amplifiers. The degradation in ASNR is found to be as large as a factor of 3. It is pointed out that mismatching would not be purposely done but can accidentally

The GS-13 with the MAT-02 Using Three Circuit Configurations

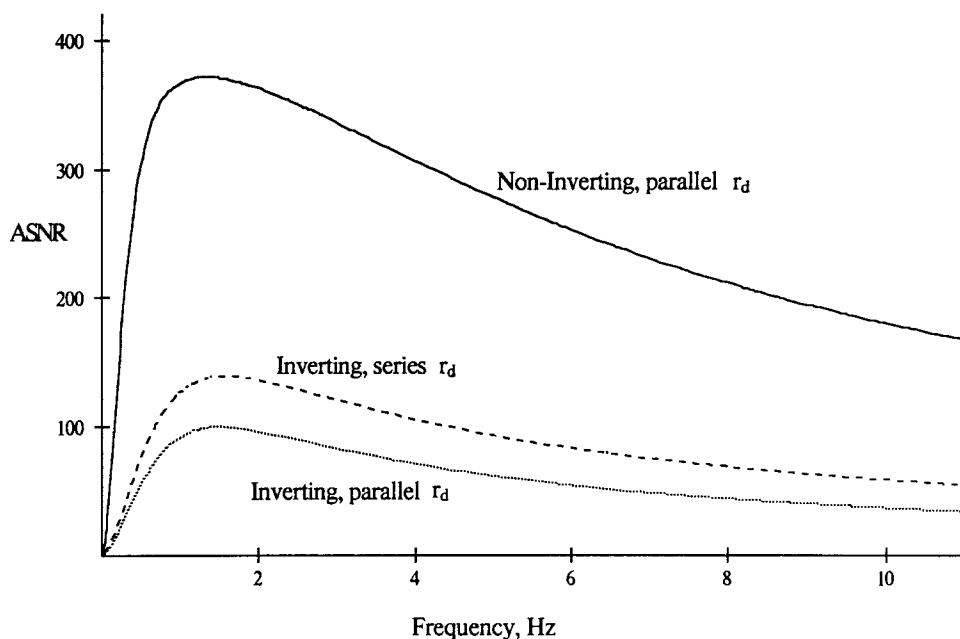


FIG. 11. This figure compares the ASNRs resulting from the three circuits shown in Figure 10. The calculations for all three circuits use the GS-13 paired with the MAT-02 with $I_c = 60 \mu\text{A}$. The lower, dotted curve is for the upper circuit in Figure 10 in which the damping resistor is in parallel with the seismometer and the inverting configuration is used for the op-amp. The middle, dashed curve applies to the middle circuit in Figure 10, in which the damping resistor is in series, and the inverting configuration is used. The upper, solid curve is for the bottom circuit in Figure 10 in which the damping resistor is in parallel, and the noninverting configuration is used. These data confirm that the parallel damping resistor, noninverting configuration results in the best ASNR. Although these calculations are for the three single-ended circuits, the same result would apply to their double-ended (differential) equivalents.

occur when connecting an EM seismometer to a seismic recorder whose input R_n properties are unknown, as is generally the case. It is recommended that manufacturers or seismic recorders make this information available.

Finally, by means of numerical comparisons among the three single-ended op-amp circuits used as preamplifiers for EM seismometers, it is found that the parallel damping resistor, non-inverting circuit is the best to use in terms of maximizing the ASNR.

RECOMMENDATIONS

More attention should be given to realizing the maximum SNR when using EM seismometers, and it is hoped that this study will motivate correctly matching the seismometer with the preamplifier and choosing the best circuit configuration. It is also recommended that:

1. Manufacturers of seismic recorders obtain from the component manufacturers the noise characteristics of the op-amp used in the analog front end of the recorder and using these data publish the input R_n ; they should also make sure that the optimum circuit is used in terms of maximizing the SNR.

2. Manufacturers of seismometers include SFs in their specifications.
3. Further study be undertaken of amplifiers that have the desirable noise characteristics described in the body of the study.

ACKNOWLEDGMENTS

This study was motivated by the author's participation in the Advanced Sensor Development Project directed by Phil Harben at the Lawrence Livermore National Laboratory. Helpful discussions were provided by Phil Harben and Steve Hunter of that laboratory, Tom McEvilly of the University of California at Berkeley, and Scott Swain of the Institute for Crustal Studies, University of California at Santa Barbara.

The analytical and numerical computations, and the graphs were made using Prescience's Theorist, Version 1.11. The manuscript benefited from careful editing by Susan Stull and Mary Boyken and the helpful suggestions of anonymous reviewer. The author wishes to acknowledge support from the Southern California Earthquake Center under Contract Number 572726 and the Lawrence Livermore National Laboratory under DOE Contract W-7405-Eng-48.

REFERENCES

- Aki, K. and P. Richards (1980). *Quantitative Seismic Theory and Methods*, W. H. Freeman, San Francisco.
- Horowitz, P. and W. Hill (1989). *The Art of Electronics*, Cambridge University Press, Cambridge.
- Peterson, J. (1982). GDSN enhancement studies final report, ARPA Order No. 4259, USGS Albuquerque Seismological Laboratory, Albuquerque, New Mexico.
- Peterson, J. and C. Hutt (1982). *Test and calibration of the Digital World-Wide Standardized Seismograph*, U.S. Geol. Surv. Open-File Rep. 82-1087.
- Peterson, J. and C. Hutt (1989). *IRIS/USGS plans for upgrading the Global Seismographic Network*, U.S. Geol. Surv. Open-File Rep. 89-471.
- Peterson, J. and E. T. Tilgner (1985). *Description and preliminary testing of the CDSN sensor systems*, U.S. Geol. Surv. Open-File Rep. 85-288.
- Riedesel, M. A., R. A. Moore, and J. A. Orcutt (1990). Limits of sensitivity of inertial seismometers with velocity transducers and electronic amplifiers, *Bull. Seism. Soc. Am.* **80**, 1725-1752.
- Rodgers, P. W. (1975). A note on the nonlinear response of the pendulous accelerometer, *Bull. Seism. Soc. Am.* **65**, 523-530.
- Rodgers, P. W. (1992). Frequency limits for seismometers as determined from signal-to-noise ratios. Part 1. The electromagnetic seismometer, *Bull. Seism. Soc. Am.* **82**, 1071-1098.
- Tobey, G. E., J. G. Graeme, and L. P. Huelsman (1971). *Operational Amplifiers: Design and Applications*, McGraw-Hill, New York.

APPENDIX A

The Relationship between Coil Resistance and Damping Resistance

The equation of motion for an EM seismometer that has current damping due to a current, i , flowing through a damping resistor, r_d , across its terminals is given by

$$M\ddot{z} + B\dot{z} + Kz = M\ddot{x} - f_d, \quad (\text{A1})$$

where x is the frame displacement, z is the relative displacement between the mass and the frame, M is the mass, B is the mechanical damping, K is the spring constant, and f_d is the force due to the damping current. This damping current has a value given by

$$i = \frac{G\dot{z}}{r_c + r_d}, \quad (\text{A2})$$

where G is the open circuit generator constant previously defined for equation (1). The coil resistance is r_c . The force on the mass due to the damping current is found from

$$f_d = Gi = \frac{G^2}{r_c + r_d} \dot{z}. \quad (\text{A3})$$

Substitute this expression for f_d into the equation of motion, equation (A1) to obtain

$$\ddot{z} + (2\zeta_0\Omega + 2\zeta_i\Omega)\dot{z} + \Omega^2 z = \ddot{x}, \quad (\text{A4})$$

in which

$$2\zeta_0\Omega = \frac{B}{M} \quad (\text{A5})$$

and

$$2\zeta_i\Omega = \frac{1}{M} \frac{G^2}{r_c + r_d}. \quad (\text{A6})$$

In equation (A6), ζ_o is the open circuit damping ratio, and ζ_i is the current damping ratio. From equation (A6), the current damping ratio is found to be

$$\zeta_i = \frac{1}{4\pi} \cdot \frac{C^2}{Mf_o} \cdot \frac{r_c}{r_c + r_d}, \quad (\text{A7})$$

where f_o and C are obtained from the previously defined relationships:

$$\Omega = 2\pi f_o, \quad (\text{A8})$$

and

$$G^2 = C^2 r_c. \quad (\text{A9})$$

Finally, the total damping, ζ , in the seismometer is made up of the sum of the open circuit damping and the current damping:

$$\zeta = \zeta_o + \zeta_i. \quad (\text{A10})$$

Now, for a given value of ζ , find the relationship between r_c and r_d by substituting ζ_i from equation (A7) into equation (A10) above and solving for r_d . This results in the desired relationship, which was used in equation (8) in the body of the study:

$$r_d = \left(\frac{C^2}{4\pi M f_o (\zeta - \zeta_o)} - 1 \right) \cdot r_c. \quad (\text{A11})$$